

Supporting Information

Transient Resonance Raman Spectroscopy of a Light-Driven Sodium-Ion-Pump Rhodopsin from *Indibacter alkaliphilus*

Kousuke Kajimoto,[†] Takashi Kikukawa,^{‡,||} Hiroki Nakashima,[†] Haruki Yamaryo,[†]
Tomotsumi Fujisawa,[†] Makoto Demura,^{‡,||} and Masashi Unno[†]

[†]Department of Chemistry and Applied Chemistry, Graduate School of Science and Engineering, Saga University, Saga 840-8502, Japan, [‡]Faculty of Advanced Life Science, Hokkaido University, Sapporo 060-0810, Japan, ^{||}Global Station for Soft Matter, Global Institution for Collaborative Research and Education, Hokkaido University, Sapporo 060-0810, Japan

1. Supplemental Figures

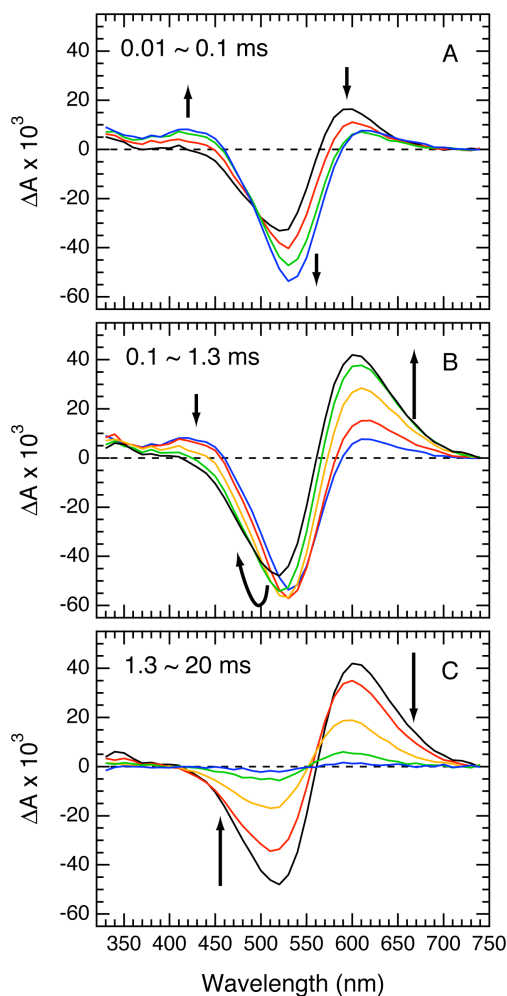


Figure S1. Transient flash-induced absorption changes of NaR from *Indibacter alkaliphilus* in three different time ranges.

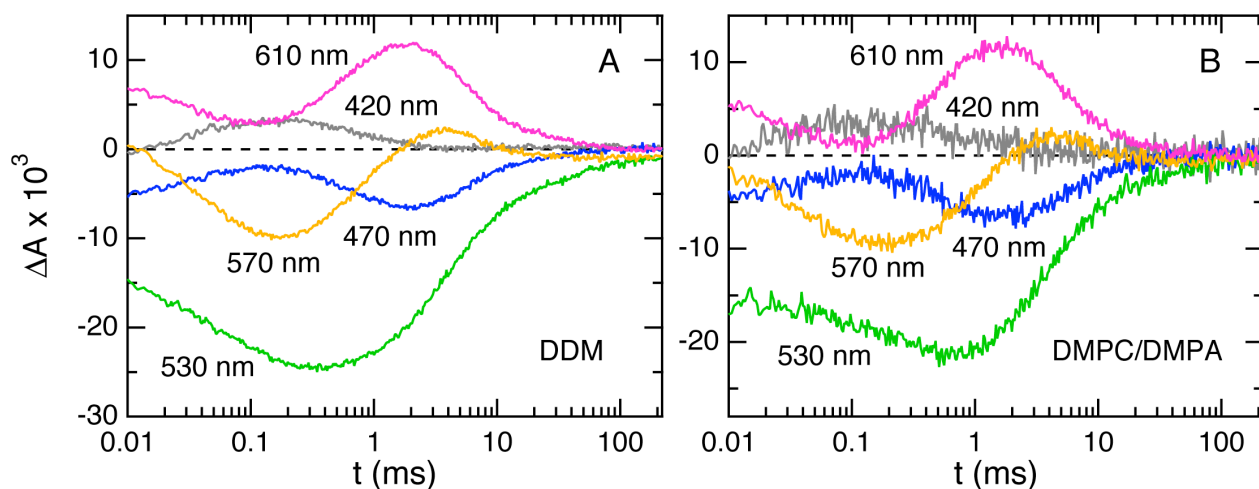


Figure S2. Transient flash-induced absorption changes of NaR from *I. alkaliphilus*. Measurements were performed at 25°C in 50 mM Tris-HCl, pH 7.0, 0.2 M NaCl. (A) NaR was solubilized by 0.05% DDM. (B) NaR was reconstituted with a 9:1 (w/w) mixture of 1,2-dimyristoyl-sn-glycero-3-phosphocholine/1,2-dimyristoyl-sn-glycero-3-phosphate (DMPC/DMPA) at 1:20 protein-to-lipid (Mole fraction) ratio.

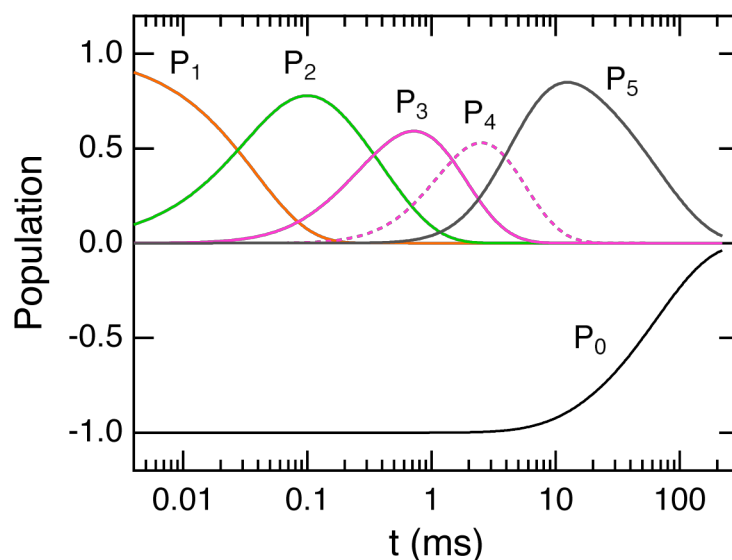


Figure S3. Time-dependent population changes of P_0 – P_5 states. P_0 is the initial dark state, whereas P_1 – P_5 are the kinetically defined states calculated by global fitting.

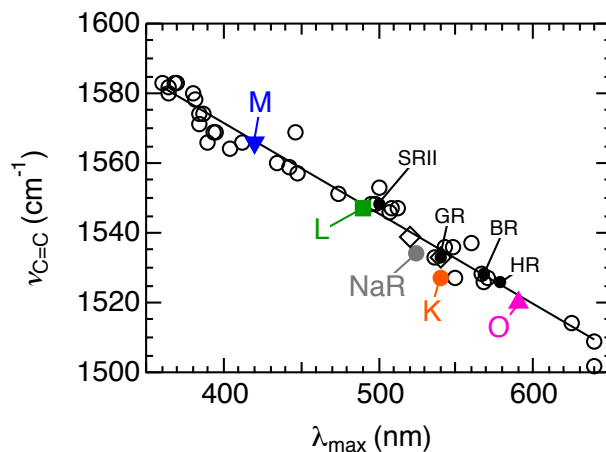


Figure S4. Plot of the observed ethylenic stretching frequency $\nu_{C=C}$ and the absorption maximum λ_{max} of retinal proteins and model compounds. The closed symbols in black represent data for the light-adapted BR, HR from *Natronomonas pharaonis*, GR, and SR11 from *Natronomonas pharaonis*.¹ The colored symbols are data for NaR from *Indibacter alkaliphilus*: dark state NaR (black), K (orange), L (green), M (blue), and O (magenta). The open circles are data for several retinal proteins and model compounds taken from Ref 1 and Ref 2.

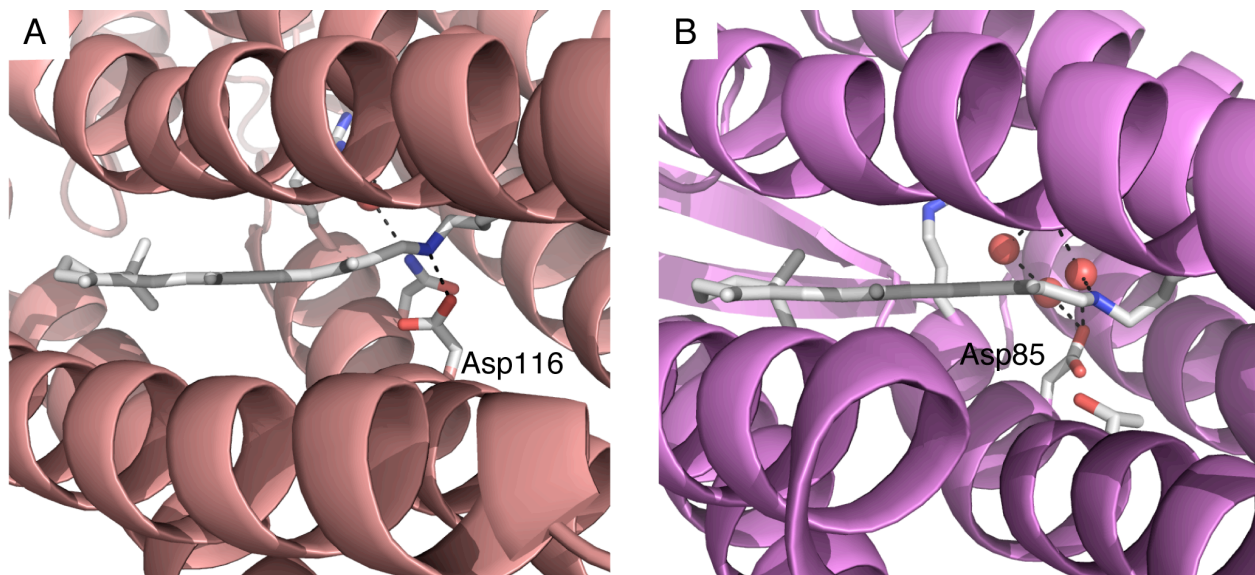


Figure S5. Structural differences in the all-trans retinal chromophore between NaR (KR2) and BR. The active site structures of (A) KR2 and BR based on their crystal structure. PDB codes: 3X3C (KR2) and 1C3W (BR).

Table S1. Selected Dihedral Angles of the Retinal Chromophore for NaR (KR2), BR, PR, and SRII

	C6-C7	C7-C8	C8-C9	C9-C10	C10-C11	C11-C12	C12-C13	C13-C14	C14-C15	C15-N
KR2, 3X3C ^a	-170.2	176.9	174.3	177.2	-179.1	167.49	-166.7	169.4	162.5	142.0
KR2, 3X3B ^b	179.9	178.5	-178.6	178.8	-179.1	174.1	-172.0	179.7	-177.3	137.5
KR2, 4XTL ^c	-178.7	176.7	-179.8	-177.7	-174.1	169.88	177.7	174.9	-173.1	137.1
KR2,4 XTN ^d	-179.5	179.4	-179.9	-178.3	-169.5	164.08	-179.2	179.4	177.7	139.6
KR2, 4XTO ^e	179.9	-179.8	-179.8	-179.7	-160.9	-172.41	-179.6	179.9	174.0	125.1
BR, 1C3W ^f	176.3	175.2	-173.7	-178.5	178.8	178.9	177.6	-156.9	179.0	-162.7
GPR, 2L6X ^g	175.5	176.7	-158.1	-176.8	177.2	-176.0	-170.7	-173.4	-169.6	-166.4
BPR, 4JQ6 ^h	179.3	-179.7	179.9	-179.9	-179.6	179.7	179.8	-179.9	-179.4	-171.5
SRII, 1H68 ⁱ	177.9	179.9	177.6	-179.2	177.6	-178.3	178.1	-179.4	179.1	-143.4

^aKR2 at pH 4.0. Ref. 3. ^bKR2 at pH 7.5–8.5. Ref. 3. ^cType A KR2 crystal in Ref. 4. pH 4.3. ^dType B KR2 crystal in Ref. 4. pH 4.9. ^eType C KR2 crystal in Ref. 4. pH 5.6. ^fThe crystal structure of BR, Ref. 5. ^gThe green-light absorbing PR solved by solution NMR spectroscopy. Ref. 6. ^hThe crystal structure of blue-light absorbing PR. Ref. 7. ⁱThe crystal structure of SRII from *Natronomonas pharaonis*, Ref. 8.

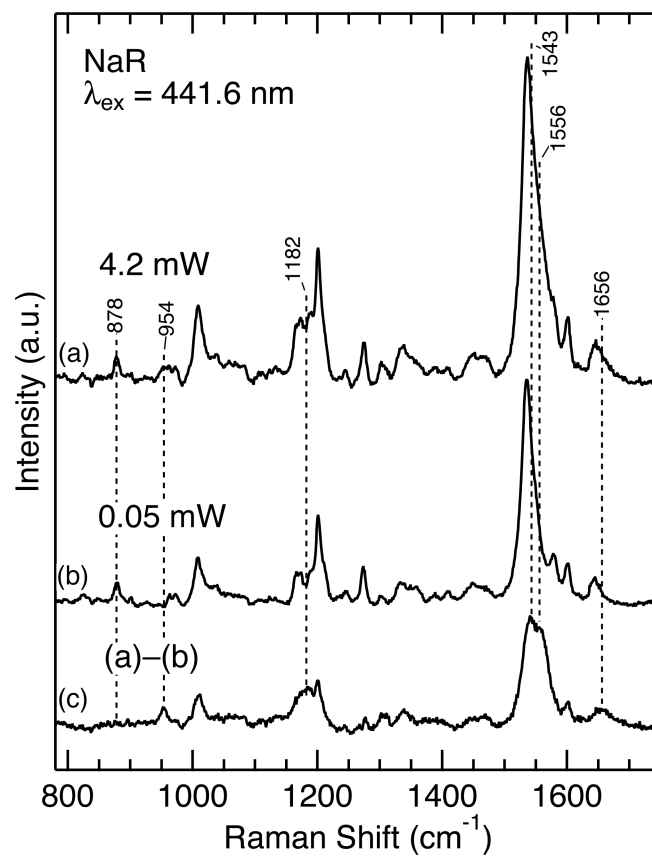


Figure S6. Transient resonance Raman spectra of photointermediates for NaR from *Indibacter alkaliphilus*. The excitation wavelength was 441.6 nm, and the medium was 50 mM Tris-HCl buffer, 400 mM NaCl, and 0.05% DDM at pH 8.0.

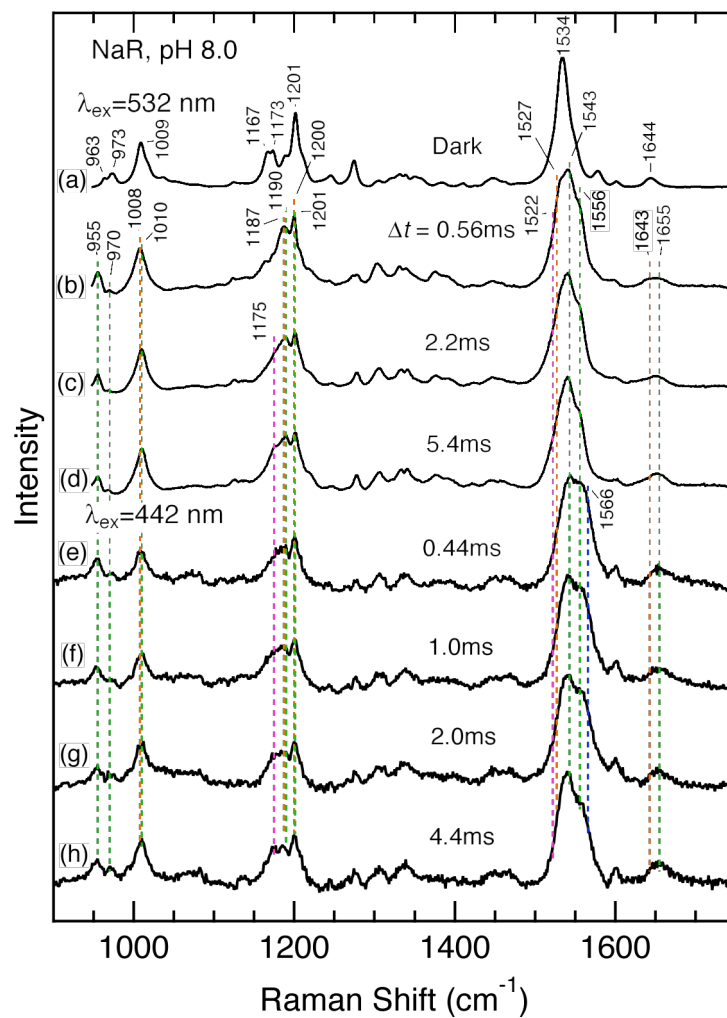


Figure S7. Transient resonance Raman spectra of NaR from *Indibacter alkaliphilus* with 532 nm (a–d) and 441.6 nm (e–h) excitation.

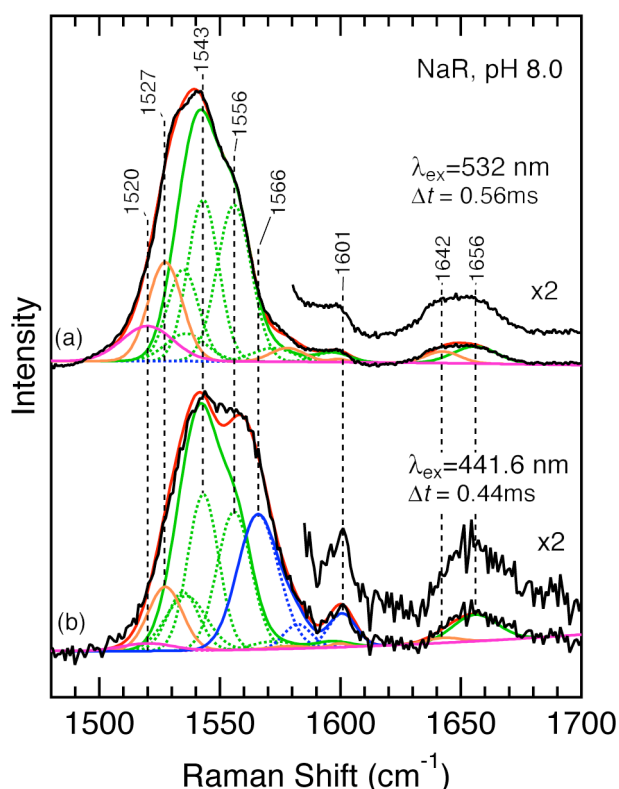


Figure S8. A global fitting analysis of the transient resonance Raman spectra of NaR from *Indibacter alkaliphilus*. (a) $\lambda_{\text{ex}} = 532$ nm, $\Delta t = 0.56$ ms. (b) $\lambda_{\text{ex}} = 441.6$ nm, $\Delta t = 0.44$ ms. The magnified spectra are also displayed in the C=N stretching region. The spectra for K (orange), L (green), M (blue), and O (magenta) intermediates are shown. Dotted lines represent the individual Gaussian band shape components.

2. Supplemental Experimental Section

Expression and Purification of IaNaR

Escherichia coli (*E. coli*) strain DH5 α was used for DNA manipulation. The IaNaR gene (GenBank accession number: EOZ93469) was amplified by PCR from the genomic DNA of *Indibacter alkaliphilus* KCTC 22604 and firstly ligated to the *Nde*I/*Xho*I site of the pET-21c (+) vector (Merck). This plasmid encodes IaNaR having additional amino acids in the C-terminus (-LEHHHHHH). Next, the IaNaR coding region was amplified by PCR while introducing the *Hind*III site after the stop codon. The resultant DNA fragment was inserted into the pKA001 vector under the lacUV5 promoter with *Nde*I and *Hind*III sites.⁹ The DNA sequence was confirmed by a standard procedure using an automated DNA sequencer (model 3100, Applied Biosystems, Foster City, CA, USA).

E. coli strain BL21 was used for the expression and purification of IaNaR. The procedures were essentially the same as the ones previously described.¹ Briefly, the cells harboring the pKA001 vector were grown in 2 \times YT medium at 37°C, and expression was induced by the addition of 1 mM isopropyl- β -D-thiogalactopyranoside in the presence of 10 μ M all-trans retinal.

After 4 h of induction, the cells were harvested and broken with a French press. The collected cell membrane fraction was solubilized with 1.5% n-dodecyl β -D-maltopyranoside (DDM) (Dojindo Lab., Kumamoto, Japan), and the solubilized IaNaR was purified using Ni-NTA agarose (Qiagen, Hilden, Germany). The yield of IaNaR was approximately 30 mg from 1 L culture. The concentration of IaNaR was determined from the absorbance at 525 nm with an assumed extinction coefficient of $50,000 \text{ M}^{-1} \text{ cm}^{-1}$.

Determination of the P_0 Spectrum

The absorption spectrum of P_0 state was determined from the measured spectrum of the dark state and used for the spectral calculations of the P_i states in Figure 3. The procedures were shown in Figure S9. Besides the scattering background, the measured spectrum (black line in the inset) includes three absorption bands: main band around 525 nm, β -band around 400 nm and the band from the aromatic amino acid residues around 280 nm. For the same analyses in the previous reports,¹ we used the sum of former two bands as the P_0 spectrum. However, the presence of β -band often confuses the appearance of short wavelength intermediates in the P_i states. Here, we estimated the main band and used as the P_0 spectrum. Firstly, we estimated the scattering background (red broken line in the inset) by the term of α / λ^4 (λ in nm). The determined value of α was 1.43×10^9 . This scattering curve was subtracted from the measured spectrum. For the resultant spectrum (red solid line), we estimated the β -band (blue line) by the skewed Gaussian function, which is defined by the four parameters: λ_{max} (in nm), A_{max} (amplitude at λ_{max}), ρ (skewness of the band) and $\Delta\nu$ (half-bandwidth in cm^{-1}).¹⁰ The determined values were $\lambda_{\text{max}} = 380 \text{ nm}$, $A_{\text{max}} = 0.057$, $\rho = 1.34$, and $\Delta\nu = 5345 \text{ cm}^{-1}$, respectively. Then, the main band (black line) was calculated by subtracting the β -band from the spectrum shown in red solid line.

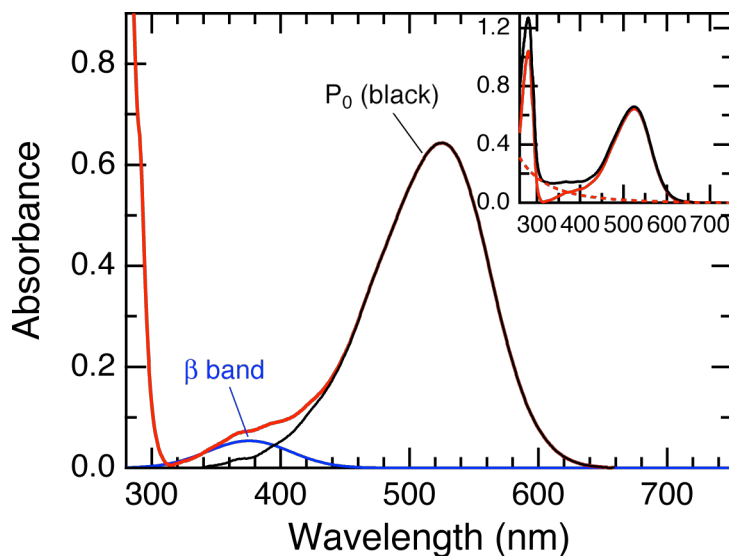


Figure S9. Determination of the P_0 spectrum. The main absorption band around 525 nm (black line) was calculated by subtracting the scattering background (broken line in the inset) and the β -band (blue line) from the measured absorption spectrum of the dark state (black line in the inset), and then used as the P_0 spectrum (for details see text).

References

- (1) Tateishi, Y.; Abe, T.; Tamogami, J.; Nakao, Y.; Kikukawa, T.; Kamo, N.; Unno, M. Spectroscopic Evidence for the Formation of an N Intermediate during the Photocycle of Sensory Rhodopsin II (Phoborhodopsin) from *Natronobacterium pharaonis*. *Biochemistry* **2011**, *50*, 2135–2143.
- (2) Heyde, M. E.; Gill, D.; Kilponen, R. G.; Rimai, L. Raman Spectra of Schiff Bases of Retinal (Models of Visual Photoreceptors). *J. Am. Chem. Soc.* **1971**, *93*, 6776–6780.
- (3) Kato, H. E.; Inoue, K.; Abe-Yoshizumi, R.; Kato, Y.; Ono, H.; Konno, M.; Hososhima, S.; Ishizuka, T.; Hoque, M. R.; Kunitomo, H.; et al. Structural Basis for Na⁺ Transport Mechanism by a Light-Driven Na⁺ Pump. *Nature* **2015**, *521*, 48–53.
- (4) Gushchin, I.; Shevchenko, V.; Polovinkin, V.; Kovalev, K.; Alekseev, A.; Round, E.; Borshchevskiy, V.; Balandin, T.; Popov, A.; Gensch, T.; Fahlke, C.; Bamann, C.; Willbold, D.; Buldt, G.; Bamberg, E.; Gordeliy, V. Crystal Structure of a Light-Driven Sodium Pump. *Nat. Struct. Mol. Biol.* **2015**, *22*, 390–395.
- (5) Luecke, H.; Schobert, B.; Richter, H. T.; Cartailler, J. P.; Lanyi, J. K. Structure of Bacteriorhodopsin at 1.55 Å Resolution. *J. Mol. Biol.* **1999**, *291*, 899–911.
- (6) Reckel, S.; Gottstein, D.; Stehle, J.; Lohr, F.; Verhoefen, M. K.; Takeda, M.; Silvers, R.; Kainosho, M.; Glaubitz, C.; Wachtveitl, J.; Bernhard, F.; Schwalbe, H.; Guntert, P.; Dotsch, V. Solution NMR Structure of Proteorhodopsin. *Angew. Chem. Int. Ed.* **2011**, *50*, 11942–11946.
- (7) Ran, T.; Ozorowski, G.; Gao, Y.; Sineshchekov, O. A.; Wang, W.; Spudich, J. L.; Luecke, H. Cross-Protomer Interaction with the Photoactive Site in Oligomeric Proteorhodopsin Complexes. *Acta Crystallogr. Sect. D* **2013**, *69*, 1965–1980.
- (8) Royant, A.; Nollert, P.; Edman, K.; Landau, E. M.; Pebay-Peyroula, E.; Navarro, J. X-ray Structure of Sensory Rhodopsin II at 2.1-Å Resolution. *Proc. Natl. Acad. Sci. USA* **2001**, *98*, 10131–10136.
- (9) Lee, K. A.; Lee, S. S.; Kim, S. Y.; Choi, A. R.; Lee, J. H.; Jung, K. H. Mistic-fused Expression of Algal Rhodopsins in *Escherichia coli* and its Photochemical Properties. *Biochim. Biophys. Acta* **2015**, 1850, 1694–1703.
- (10) Chizhov, I.; Chernavskii, D. S.; Engelhard, M.; Mueller, K. H.; Zubov, B. V.; Hess, B. Spectrally Silent Transitions in the Bacteriorhodopsin Photocycle. *Biophys. J.* **1996**, *71*, 2329–2345.